Applied Mathematics & Information Sciences
An International Journal

http://dx.doi.org/10.18576/amis/150111

A Deep Neural Approach for Real-Time Malignant Melanoma Detection

Samy Bakheet[1,*] *and Aml El-Nagar*[2]

[1]Department of Information Technology, Faculty of Computers and Information, Sohag University, P. O Box 82533 Sohag, Egypt
[2]Department of Mathematics and Computer Science, Faculty of Science, Sohag University, P. O Box 82524 Sohag, Egypt

Received: 28 Aug. 2020, Revised: 24 Oct. 2020, Accepted: 11 Nov. 2020
Published online: 1 Jan. 2021

Abstract: Recently, several potentially useful computer-aided diagnosis (CAD) systems have become feasible and are now used widely to help physicians in automated cancer detection and grading from dermoscopy images. In this paper, we present a real-time CAD framework using a deep neural network (DNN) for fine-grained classification and grading in dermoscopic skin cancer images. The input skin image is first preprocessed for removing the noise and enhancing the image quality. An adaptive segmentation scheme based on the well-established Otsu thresholding method is performed to accurately extract suspected skin lesion regions from the enhanced input image. Then, a reduced set of visual features is extracted based on both color and typical geometric properties of skin lesions. Finally, the selected lesion features are fed as inputs into a rapid DNN classifier for classifying each lesion in a given dermoscopic image as a benign or melanoma lesion. On the publicly available PH2 dermoscopy imaging dataset, the proposed method is successfully tested and validated, achieving 97.5%, 96.67% and 100.0% for average diagnostic accuracy, sensitivity and specificity, respectively. These results compare quite favorably with those obtained from more sophisticated state-of-the-art approaches.

Keywords: CAD, Dermoscopic image, Dermoscopy, Melanoma skin cancer, DNN.

1 Introduction

The National Cancer Institute (NCI) reported that skin cancer is the most common type of cancer (the most serious form). The main types of skin cancer are squamous cell carcinoma, basal cell carcinoma, and melanoma. Melanoma is much less common than other types, but much more likely to invade nearby tissue and spread to other parts of the body. Most deaths from skin cancer are caused by melanoma. Moreover, it is most frequently diagnosed among people aged 65-74 and the percentage of its subsequent deaths is highest among people aged 75-84. It is estimated that there will be 100,350 new cases of melanomas and 6,850 deaths in 2020 [1]. Melanoma is a skin cancer that has harmed DNA (mutations) in skin cells, causing uncontrolled growth of these cells. Developments from the melanocyte (a melanin-producing cell) are located in the stratum basal of the epidermis. It normally occurs in the skin, but may rarely occur in the eye, intestines, or mouth. The main known exogenous risk factor for melanoma is exposure to ultraviolet radiation. Meantime, a personal history of sunburn, giant congenital nevi, genetic mutations, and a case history of melanoma all increase the risk of developing melanoma.

An important method to assist within the diagnosis of melanotic lesions is Epiluminescence Microscopy (ELM), also known as dermatoscopy [2, 3] allows for the magnification of lesions while simultaneously providing a polarized light source rendering the stratum cornea translucent. Dermoscopy is considered more effective than clinical melanoma diagnosis in pigmented skin lesions. The diagnostic accuracy of dermoscopy is largely dependent on dermatology training.

Throughout time, several clinical rules devised by dermatologists have been established to classify skin lesions. Some of these methodologies are the Pattern Analysis [4], ABCD rule [5], Menzies method [6], and 7-point checklist [7]. A vision-based system typically requires three main processes for automatically detection of melanoma skin cancer: (i) preprocessing and lesion segmentation, (ii) extraction and selection of the features, and (iii) classification of the lesions. The first step involves obtaining pre-processing the skin lesion image using noise filtering, such as removing salt-and-pepper

* Corresponding author e-mail: samy.bakheet@fci.sohag.edu.eg

noise and enhancing the image. Afterwards, lesion segmentation is applied to isolate only the region of interest (ROI) from the surrounding healthy skin.

During the extraction process, a series of specific dermoscopic characteristics similar to those visually recognized by specialist dermatologists, such as asymmetry, border irregularity, color, differential structures, etc. is defined and extracted from the segmented region of the lesion to accurately describe a melanoma lesion. Finally, the skin lesion features extracted are fed into the feature classification module to classify skin lesions into one of two different categories: malignant or benign. The remainder of the paper is organized, as follows: Section 2 covers some related work on skin cancer detection. In Section 3, the proposed method is described in detail. Experimental results are reported are discussed in Section 4. Section 5 is devoted to conclusions and future directions.

2 Related Work

A newly released report by the World Health Organization (WHO) has estimated that the average annual number of new diagnosed invasive melanoma cases has increased by nearly 47 percent worldwide during the past decade. That is why a lot of researchers in the field of computer vision and medical imaging have been highly interested and enthusiastic about CAD modelling, and they have exerted a lot of effort in the last years to develop high performance methods and technologies for automatic skin cancer detection from dermoscopy images [8, 9].

Accurate skin lesion segmentation is a crucial early step in the analysis of lesion images, and the segmentation is very challenging because of factors such as color variations, irregular structural, illumination variations, the presence of hair, as well as multiple lesions in the skin [10–13]. Many algorithms have been proposed to automatically segment skin lesion images, including histogram thresholding [14, 15], clustering [16, 17], active contours [18, 19], edge detection [20, 21], graph theory [22], and probabilistic modeling [23]. Feature extraction is most vital for the classification and diagnosis processes of melanoma. The most common approach for identifying the physical characteristics of melanoma is a rule mentioned as ABCD skin cancer [24]. In [25], the authors proposed a melanoma recognition system using support vector machine classifier, and the features detected are based on asymmetry, border irregularity, color variation, diameter and texture of the lesion. Another related work is [26], where the author proposed a system for melanoma skin cancer detection and classification using an SVM classification model and an optimized set of HOG-based descriptors of skin lesions.

3 Proposed Methodology

The proposed approach for detecting skin cancer with melanoma is described in this section. Fig.1 shows a brief conceptual block diagram of the approach. The general structure of our proposed framework works as follows: As an initial step, the skin lesion region that is suspected of being a melanoma lesion is first segmented from the healthy skin around, by applying iterative automatic thresholding and morphological operations. Then, a set of features is extracted from the skin lesion region. A one-dimensional vector representation is then generated from the extracted features and fed into a fast DNN classifier for skin lesion classification. The DNN classifier is trained on a dataset comprised of both melanoma and other benign skin lesion images taken from different patients. Finally, the trained DNN model is used to classify each previously unseen skin lesion as a benign or malignant lesion in a dermatoscopic image. The details of each part of our method are described within the remainder of this section.

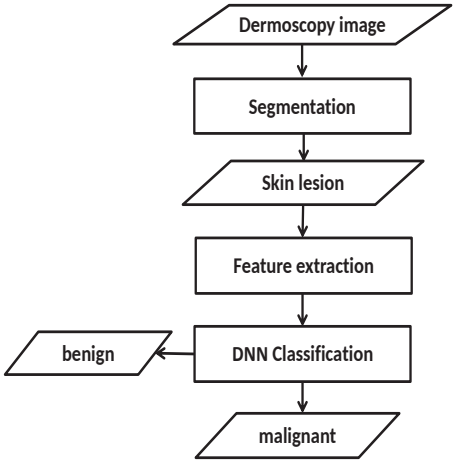

Fig. 1: Block flow diagram of the proposed methodology for melanoma skin cancer detection.

3.1 Image Pre-processing

Preprocessing stage is responsible for detecting and reducing the amount of artifacts from the image. In dermoscopy images, this step is necessary since many dermoscopy images contain a lot of noise such as skin lines, air bubbles and hair which are covering the lesion area. Incorrect segmentation of pigmented lesion can be obtained if these artifacts are not removed. Therefore, it is necessary to reduce the noise levels to increase image quality. Here, the pre-processing step involves three main

operations: (i) image resizing and grayscale conversion, (ii) noise removed by applying a simple 2D smoothing filter and (iii) image enhancement.

3.2 Skin Lesion Segmentation

Lesion segmentation is an important part of computer-based skin cancer detection. For the segmentation of skin lesions in the input image, our method involves iterative automatic thresholding and masking operations, which are applied to the enhanced input skin lesion images. The procedure begins with applying automatic thresholding proposed by Otsu method [27] for each of the R, G and B planes in the input image. Then, binary masks for each plane are obtained and then combined to create a final lesion mask. We use 3-plane masking procedure to increase segmentation accuracy. The segmented image may include other smaller blobs which are not the skin lesions. To overcome this problem, a common solution is to employ morphological-area opening [28] on the segmented image. Finally , the final segmented area containing only the skin lesion can be estimated by smoothing the binary image with a series of gradually decreasing filter sizes using an iterative median filter technique (i.e., $7 \times 7, 5 \times 5$ and 3×3).

In addition, to avoid the detection of extremely small non-skin lesions and confusion between isolated artifacts and objects of interest, we take extra precautions by applying two additional filters to ensure that they correspond to skin lesions of interest. First, an adaptive morphological open-close filter is applied iteratively to the resulting binary image to remove objects that are too small from the binary image while holding large objects in shape and size. This filter is ideally carried out using a cascade of erosion and dilation operations using locally adaptive structuring elements. The so-called size filter is used as a second filter to remove objects less than a specified size. Once the size filter is applied, almost all spurious artifacts of less than 5% of the image size will be erased from the binary image. However, all contours are detected by applying a modified canny edge detector [29] after filtering out of all unnecessary image elements and isolated objects. As shown in Fig. 2, the proposed method can produce very accurate segmentation of the skin lesion from the healthy skin surrounding it.

3.3 Feature Extraction

In this step, the most important features are extracted from the segmented lesion image. The extracted features involve color features and shape-based features. These features were checked together with various combinations, which would eventually be beneficial for the current task of skin cancer detection. A compact set of

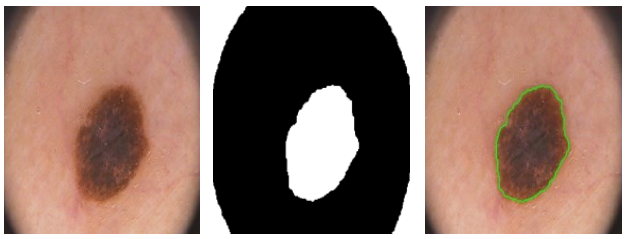

(a) Original image (b) Binary mask (c) Traced lesion

Fig. 2: The results of segmentation methodology applied to the input image.

statistical features that provides some geometrical properties of segmented lesion regions is used, including area, major axis, minor axis, perimeter, diameter and region roundness. In this work, a reduced set of geometrical features is employed, which is given as follows,

Area: The lesion area is the number of pixels of the skin lesion.

Asymmetry: The pigment is considered asymmetric, i.e., no matching halves will be produced by a line drawn through the middle. Common moles are round and symmetrical (see Fig.3).

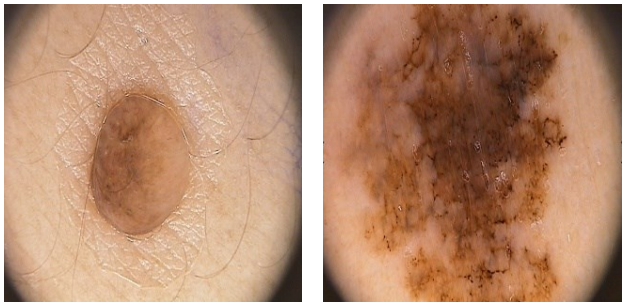

(a) Benign (b) Malignant

Fig. 3: Asymmetry of melanoma compared with benign lesion.

Diameter of the lesion: Diameter is one of the simplest and traditional methods of determining whether the segment is malignant or not by considering the length of the major axis in the best fit ellipse. A lesion is considered as malignant, if the diameter is greater than 6 mm [30].

Color variation: The skin lesion color differs over the various shades of brown, black, red, white or blue. The value of one is assigned to the presence of each color in the lesion image [30].

Compactness: This feature is also called Roundness, which describes the degree of regional shape close to

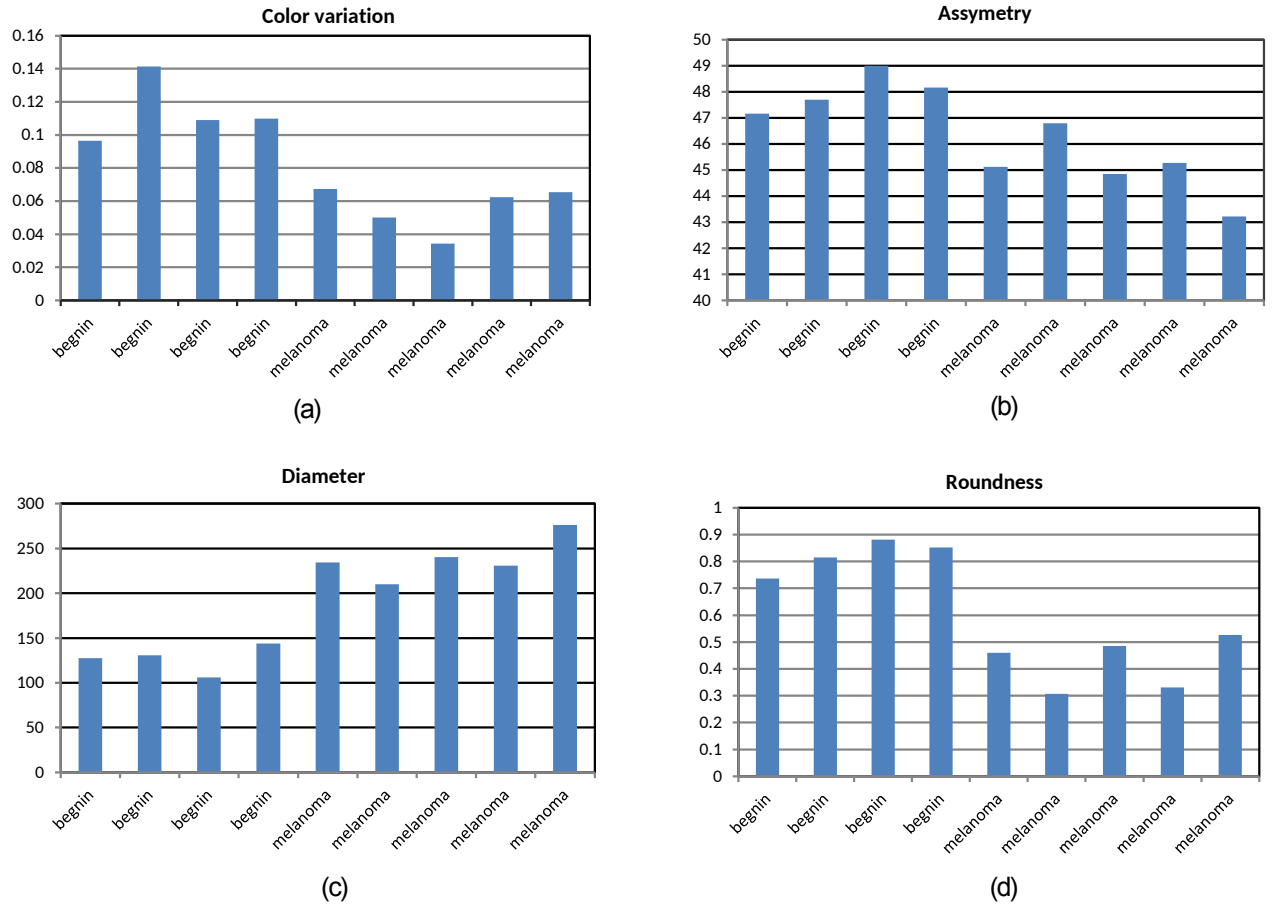

Fig. 4: Bar plots for the distribution of sample features extracted from various skin lesion images.

circular. With the size of the ROI unchanged, the region and the length of the border are often used to describe the target shape. The smaller the perimeter for fixed-area images, the closer target to the circle is. The longer the perimeter, the smoother and more complex the graphic surface. The degree of shape the graphics tend to circle using roundness measurement. The roundness rule is given as follows,

$$C = \frac{4\pi A}{P^2} \tag{1}$$

In the above formula, P and A denote the area boundary perimeter and the regional area, respectively. When the region is circular, C has the maximum value of 1, whereas when it is a long and thin strip or more complex, the C value is less than 1. Fig. 4 displays the bar plots for the distribution of some statistical features extracted from various skin lesion images.

3.4 Skin Lesion Classification

In this section, we describe the feature classification module that we used in our automatic skin lesion detection system to produce the final detection results. The classification module aims to discern the extracted features from images into malignant and benign melanoma, which is based primarily on the availability of a collection of skin lesions previously identified or classified. In this case, this set of pigmented skin lesions is called the training set and the resulting learning strategy is supervised learning.

There are numerous accurate classification methods developed in literature using learning algorithms for the automatic classification of pigmented skin lesions, such as Naïve Bayesian (NB), k-Nearest Neighbor (k-NN), Support Vector Machines (SVMs), Neural Networks (NNs), Conditional Random Fields (CRFs), etc [31–35]. In this work, the current skin lesion detection task is formulated as a typical binary classification problem, where there are two skin lesion classes, and the ultimate

goal is to assign each skin lesion in dermatoscopic images a suitable diagnostic class label (malignant melanoma or benign pigmented). There are various supervised learning algorithms [36–38] that can train a detector of malignancy of skin lesions. Because of its excellent generalization capability and reputation as a highly accurate paradigm, a DNN classification model is employed in the current detection framework. The DNN based detection model is an effective medical diagnostic approach, which consists of three layers, i.e., the input layer with five feature inputs, the three hidden layers with 24, 24, and 48 neurons taking sigmoid functions as their activation functions, and the output layer with only one neuron. Fig. 5 depicts a general schematic representation of the DNN architecture employed for fine-grained classification of dermoscopic skin cancer images.

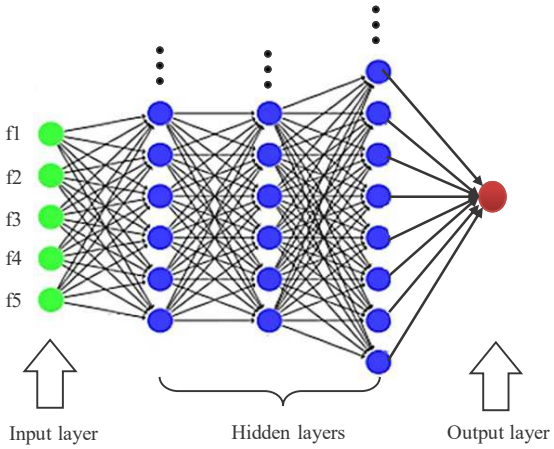

Fig. 5: A general schematic representation of the DNN architecture employed for fine-grained classification of dermoscopic skin cancer images.

In the proposed detection system, in the beginning of training, the weights are randomly initialized. There are known feature inputs and a desired output. During each trial epoch, a predicted output is generated by the deep neural model, which is compared to the desired output, and an error is produced when both outputs are not equal. This error is propagated backwards and weights are updated, such that the training is stopped when the difference between the desired output and predicted output are minimized. The classification results would have misclassification, where the classification model might identify a normal lesion as malignant melanoma, or vice versa.

4 Experimental Results

In this section, the conducted experiments are explained and their results are shown and discussed to demonstrate the performance of the proposed malignant melanoma detector. The performance of the proposed method is tested and validated on the publicly available benchmark PH2 dermoscopy dataset [39]. The dataset consists of 200 8-bit RGB dermoscopic images of melanocytic lesions with a resolution of 768×560 pixels. The images involve three types of skin lesions: 80 common nevi, 80 atypical nevi and 40 melanomas, which were obtained at the Dermatology Service of Hospital Pedro Hispano (Matosinhos, Portugal) under the same conditions through the tuebinger mole analyzer system using a magnification of 20 times. Fig. 6 shows a sample of skin lesions from the PH2 dermoscopy imaging dataset.

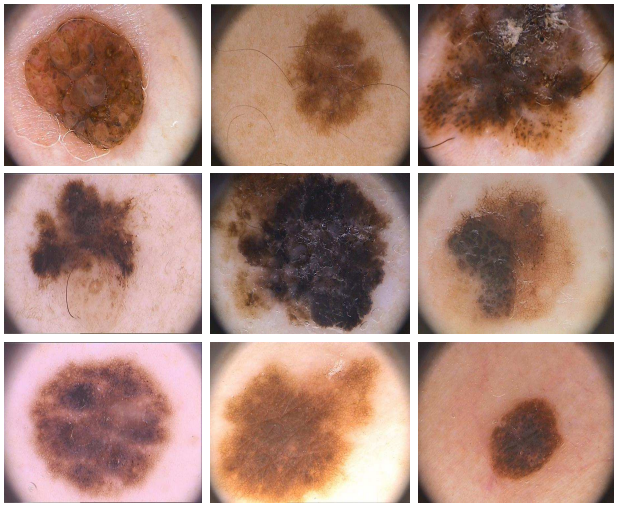

Fig. 6: A sample of skin lesions from the PH2 dermoscopy imaging dataset.

Each image was resized to a fixed size of 256×256, prior to feature extraction. The images in the dataset were randomly divided into two subsets, i.e., 80% for a training set and 20% for test set. The k-fold cross-validation technique is used to assign all images to a test set exactly once. The normalized vector of the extracted features are fed as input to a feedforward neural network for feature classification. The employed activation function is a linear function which gives an output as 0 for non-cancerous or benign and 1 for cancerous or malignant. Deep Learning Toolbox^{TM} in MATLAB® was used for creating and interconnecting the layers of the implemented DNN.

For performance evaluation, the results obtained from the proposed method are quantitatively assessed in terms of three commonly used performance indices, namely, sensitivity (SN), specificity (SP) and accuracy (AC) which are defined as follows,

Sensitivity (also called true positive rate or recall) generally refers to the ability to identify melanoma case positively, i.e,

$$SN = \frac{TP}{TP + FN} \times 100\% \quad (2)$$

Specificity (also called true negative rate) refers to how well a test recognizes patients who do not have a disease, i.e,

$$SP = \frac{TN}{TN+FP} \times 100\% \quad (3)$$

Accuracy is the probability that a randomly chosen instance (positive or negative, relevant or irrelevant) will be correct. More specifically, accuracy is the probability that the diagnostic test yields the correct determination, i.e.,

$$AC = \frac{TP+TN}{TP+TN+FP+FN} \times 100\% \quad (4)$$

where,

- –TP (True Positive): The number of predictions where the classifier correctly predicts the positive class.
- –TN (True Negative): The number of predictions where the classifier correctly predicts the negative class.
- –FP (False Positive): The number of predictions where the classifier incorrectly predicts the positive class.
- –FN (False Negative): The number of predictions where the classifier incorrectly predicts the negative class.

After training was carried out for a set of training images, the DNN was tested with an independent testing image set that consists of a total of 40 cases (i.e., 30 cancerous cases and 10 non-cancerous cases), and 5-fold cross-validation procedure was performed. For a complete cycle of a 5-fold cross-validation, the process is iterated five times until each image subset was chosen as a test set, and then the obtained results are averaged. The performance of the proposed CAD system was evaluated in terms of accuracy, sensitivity and specificity, yielding averaged rates of 97.5%, 96.67% and 100.0%, respectively. Such results indicate that the proposed CAD model not only is highly effective in detecting melanoma skin cancer, but also has the potential to compare very favorably to several existing state-of-the-art models. In order to quantify the competitive performance of the proposed approach, an experimental comparison of the performance of the system with that of several state-of-the-art baselines [26, 40] was carried out. This comparison is summarized in Table 1. It is worthwhile to mention that the above two approaches presented in [40] and [26] were evaluated on two different datasets of 40 and 224 dermoscopic imaging samples, respectively. All algorithms of the presented CAD system were implemented in MATLAB software (version R2016a). All tests and evaluations were carried out on a PC with an Intel(R) core(TM) i7-4770M CPU @2.40 GHz, 8 GB RAM , running Windows 10 Pro (64-bit Edition).

Table 1: Comparison of our methodology with other state-of-the-art baselines.

Method	SN (%)	SP (%)	AC (%)
Our method	**96.67**	**100.0**	**97.5**
Bakheet [26]	98.21	96.43	97.32
Elgamal [40]	100.0	95.00	97.00

5 Conclusion

In this paper, we have proposed a real-time CAD method for melanoma skin cancer, based on DNN for classification of pigmented skin lesions. Extensive experimental results on the publicly available PH2 dermoscopy imaging dataset demonstrated that the proposed method could perform favorably to other related state-of-the-art approaches, achieving average rates of 97.5%, 96.67% and 100.0% for accuracy, sensitivity and specificity, respectively. As prospects for future work, our intention is twofold. On the one hand, we plan to improve the feature extraction process by attempting to extract most discriminative and meaningful features from pigmented skin lesion regions, by way of combining the capabilities of several feature selection techniques. On the other hand, we intend to evaluate the presented method more extensively on more large-scale dermoscopic datasets that allows to build a more powerful and generic CAD model for melanoma skin cancer.

Acknowledgement

The authors are deeply grateful to the editor and anonymous reviewers for carefully reading of our work and for their insightful comments and suggestions that have greatly improved the quality of the paper.

Conflict of Interest

The authors declare that there is no conflict of interest regarding the publication of this paper.

References

[1] R. Siegel, K. Miller, and A. Jemal, Cancer statistics 2020, *CA: A Cancer Journal for Clinicians*, **70**, 7–30 (2020).
[2] M. Vestergaard, P. Macaskill, P. Holt, and S. Menzies, Dermoscopy compared with naked eye examination for the diagnosis of primary melanoma: a meta-analysis of studies performed in a clinical setting. *British Journal of Dermatology*, **159** (3), 669–676 (2008).
[3] S. Bakheet and A. Al-Hamadi, Computer-aided diagnosis of malignant melanoma using Gabor-based entropic features and multilevel neural networks. *Diagnostics*, **10**, 822–837 (2020).
[4] H. Pehamberger, A. Steiner, and K. Wolff, In vivo epiluminescence microscopy of pigmented skin lesions. i. pattern analysis of pigmented skin lesions. *Journal of the American Academy of Dermatology*, **17** (4), 571–583 (1987).

[5] W. Stolz, Abcd rule of dermatoscopy: a new practical method for early recognition of malignant melanoma. *Eur. J. Dermatol.*, **4**, 521–527 (1994).
[6] S. Menzies. A method for the diagnosis of primary cutaneous melanoma using surface microscopy. *Dermatologic clinics*, **19** (2), 299–305 (2001).
[7] G. Argenziano, G. Fabbrocini, P. Carli, V. De Giorgi, E. Sammarco, and M. Delfino. Epiluminescence microscopy for the diagnosis of doubtful melanocytic skin lesions: comparison of the abcd rule of dermatoscopy and a new 7-point checklist based on pattern analysis. *Archives of dermatology*, **134** (12), 1563–1570 (1998).
[8] A. Masood and A. Al-Jumaily. Computer aided diagnostic support system for skin cancer: a review of techniques and algorithms. *International journal of biomedical imaging*, (2013).
[9] K. Korotkov. *Automatic change detection in multiple skin lesions*. PhD thesis, Ph. D. Thesis, Universitat de Girona, Girona, (2014).
[10] M. Celebi, T. Mendonca, and J. Marques. *Dermoscopy image analysis*, **10**. CRC Press, (2015).
[11] M. Celebi, H. Iyatomi, G. Schaefer, and W. Stoecker. Lesion border detection in dermoscopy images. *Computerized medical imaging and graphics*, **33** (2), 148–153 (2009).
[12] I. Maglogiannis and C. Doukas. Overview of advanced computer vision systems for skin lesions characterization. *IEEE transactions on information technology in biomedicine*, **13** (5), 721–733 (2009).
[13] M. Celebi, H. Kingravi, B. Uddin, H. Iyatomi, Y. Aslandogan, W. Stoecker, and R. Moss. A methodological approach to the classification of dermoscopy images. *Computerized Medical imaging and graphics*, **31** (6), 362–373 (2007).
[14] R. Garnavi. *Computer-aided diagnosis of melanoma*. PhD thesis, (2011).
[15] M. Celebi, Q. Wen, S. Hwang, H. Iyatomi, and G. Schaefer. Lesion border detection in dermoscopy images using ensembles of thresholding methods. *Skin Research and Technology*, **19** (1), e252–e258 (2013).
[16] H. Zhou, G. Schaefer, A. Sadka, and M. Celebi. Anisotropic mean shift based fuzzy c-means segmentation of dermoscopy images. *IEEE Journal of Selected Topics in Signal Processing*, **3**, 26–34 (2009).
[17] P. Schmid. Segmentation of digitized dermatoscopic images by two-dimensional color clustering. *IEEE Transactions on Medical Imaging*, **18** (2), 164–171 (1999).
[18] H. Zhou, X.Li, G. Schaefer, M. Celebi, and P. Miller. Mean shift based gradient vector flow for image segmentation. *Computer Vision and Image Understanding*, **117** (9), 1004–1016 (2013).
[19] B. Erkol, R. Moss, R. Stanley, W. Stoecker, and E. Hvatum. Automatic lesion boundary detection in dermoscopy images using gradient vector flow snakes. *Skin Research and Technology*, **11** , 17–26 (2005).
[20] Q. Abbas, M. Celebi, I. García, and M. Rashid. Lesion border detection in dermoscopy images using dynamic programming. *Skin Research and Technology*, **17** (1), 91–100 (2011).
[21] M. Rajab, M. Woolfson, and S. Morgan. Application of region-based segmentation and neural network edge detection to skin lesions. *Computerized Medical Imaging and Graphics*, **28**, 61–68 (2004).
[22] X.Yuan, N. Situ, and G. Zouridakis. A narrow band graph partitioning method for skin lesion segmentation. *Pattern Recognition*, **42** (6), 1017–1028 (2009).
[23] M. Celebi, H. A Kingravi, H. Iyatomi, Y. Aslandogan, W. Stoecker, R. Moss, J. Malters, J. Grichnik, A. Marghoob, H. Rabinovitz, Border detection in dermoscopy images using statistical region merging. *Skin Research and Technology*, **14** (3), 347–353 (2008).
[24] Z. She, Y. Liu, and A. Damatoa. Combination of features from skin pattern and abcd analysis for lesion classification. *Skin Research and Technology*, **13** (1), 25–33 (2007).
[25] M. Ramezani, A. Karimian, and. Moallem, Automatic detection of malignant melanoma using macroscopic images. *Journal of medical signals and sensors*, **4** (4), 281 (2014).
[26] S. Bakheet. An SVM framework for malignant melanoma detection based on optimized HOG features. *Computation*, **5** (1), 4, (2017).
[27] Nobuyuki Otsu. A threshold selection method from gray-level histograms. *IEEE transactions on systems, man, and cybernetics*, **9** (1), 62–66 (1979).
[28] L. Vincent. Morphological area openings and closings for grey-scale images. *Shape in Picture*, 197–208 (1994).
[29] J. Canny. A computational approach to edge detection. *IEEE Transactions on pattern analysis and machine intelligence*, **6**, 679–698 (1986).
[30] N. Ramteke and S. Jain. Abcd rule based automatic computer-aided skin cancer detection using matlab. *International Journal of Computer Technology and Applications*, **4** (4), 691 (2013).
[31] S. Sadek, A. Al-Hamadi, B. Michaelis, and U. Sayed. An action recognition scheme using fuzzy log-polar histogram and temporal self-similarity. *EURASIP Journal on Advances in Signal Processing*, **2011** (1), 540375 (2011).
[32] S. Sadek, A. Al-Hamadi, B. Michaelis, and U. Sayed. *An svm approach for activity recognition based on chord-length-function shape features*. in Proc. 2012 19th IEEE International Conference on Image Processing, pages 765–768, (2012).
[33] S. Bakheet and A. Al-Hamadi. A discriminative framework for action recognition using f-hol features. *Information*, **7** (4), 68, (2016).
[34] S. Sadek, A. Al-Hamadi, B. Michaelis, and U. Sayed. *Human action recognition via affine moment invariants.* in Proc. of the 21st International Conference on Pattern Recognition (ICPR2012), 218–221, (2012).
[35] S. Sadek, A. Al-Hamadi, and B. Michaelis. Toward real-world activity recognition: An svm based system using fuzzy directional features. *WSEAS Trans Inf Sci Appl*, **10**, 116–127 (2013).
[36] S Sadek, A Al-Hamadi, B Michaelis, and U Sayed. *Towards robust human action retrieval in video.* in Proc. of the British Machine Vision Conference (BMVC'10), (2010).
[37] S. Sadek, A. Al-Hamadi, B. Michaelis, and U. Sayed. *Human activity recognition: a scheme using multiple cues.* in International Symposium on Visual Computing, 574–583, (2010).
[38] S Sadek, A Al-Hamadi, M Elmezain, B Michaelis, and U Sayed. *Human activity recognition using temporal shape moments.* in IEEE Int. Symposium on Signal Processing and Information Technology (ISSPIT2010), 79–84, (2010).

[39] T. Mendonça, P. Ferreira, J. Marques, A. Marcal, and J. Rozeira. *PH2 – A dermoscopic image database for research and benchmarking.* in 2013 35th annual international conference of the IEEE engineering in medicine and biology society (EMBC), 5437–5440, (2013).

[40] M. Elgamal. Automatic skin cancer images classification. *IJACSA) International Journal of Advanced Computer Science and Applications*, **4** (3), 287–294 (2013).

Samy Bakheet received the doctoral degree (Dr.-Ing.) in Neuro-Information Technology (NIT) from Otto-von-Guericke University Magdeburg (IIKT), Germany in 2013. His research interests are geared towards high-level recognition problems in machine vision, such as human activity/event recognition, human pose estimation, object/scene recognition, etc. Bakheet has authored more than 50 refereed papers in well-reputed journals and international conference/symposium proceedings in the fields of computer vision, machine learning, pattern recognition, medical imaging, CAD, and robotics.

Aml El-Nagar received her MS Degree from Sohag University in 2011. Her research interests include deep learning, machine learning, image processing, medical imaging, and computer-aided diagnosis.